Proc. Natl. Acad. Sci. USA
Vol. 86, pp. 6403–6407, August 1989
Neurobiology

Neural cell adhesion molecule (N-CAM) is elevated in adult avian slow muscle fibers with multiple terminals

(neuromuscular junction/syrinx/polyinnervation)

WILLIAM BLEISCH, CONSTANCE SCHARFF, AND FERNANDO NOTTEBOHM

Laboratory of Animal Behavior, The Rockefeller University, New York, NY 10021

Contributed by Fernando Nottebohm, May 10, 1989

ABSTRACT **Many adult avian muscles contain two types of muscle fiber: those that receive innervation at single focal terminals and those with multiple terminals. The muscles of the syrinx, the vocal organ of birds, are such mixed muscles. To study this heterogeneity of fiber type and innervation, we combined immunocytochemistry to classify muscle fibers with techniques to visualize neuromuscular junctions. One monoclonal antibody, S58, directed against a slow class of myosin, labels only fibers that have multiple terminals. We also examined the distribution of immunoreactivity for neural cell adhesion molecule (N-CAM), which has been suggested to play a role in innervation of muscle and formation of neuromuscular junctions. S58-positive fibers have elevated N-CAM staining, indicating that multiple innervation of a fiber is correlated with the fiber's expression of high levels of N-CAM immunoreactivity. Most, and perhaps all, fibers that have multiple terminals also contain abundant N-CAM immunoreactivity. This suggests that N-CAM may play a role in the maintenance of multiterminal innervation in adult innervated muscle.**

While fast-twitch muscle fibers are innervated by a single axon at a single focal terminal, many muscle fibers have a distinct pattern of innervation with multiple small terminals (1). The classic comparison of differences in muscle innervation is between the posterior and anterior latissimus dorsi muscles (PLD and ALD) in the chicken (2, 3). The PLD is a fast-twitch muscle of the wing; the ALD is an adjacent postural muscle composed of slow tonic fibers, incapable of fast contractions but able to sustain contractions for much longer than PLD fibers (3). PLD fibers have predominantly "fast" isoforms of myosin and other protein, while ALD fibers contain "slow" isoforms (see ref. 4 for review; refs. 5 and 6). In addition to differences in physiology and biochemistry, these two muscles differ in their pattern of innervation (7). Muscle fibers in the adult PLD are innervated by single motoneurons at single focal end plates, one on each fiber. ALD fibers are innervated by multiple motoneurons and have multiple small terminals scattered along their lengths. The ALD and PLD are composed almost exclusively of multiterminal and single-terminal fibers, respectively. However, there are muscles, such as the biventer cervis, the "complexus" and the sartorius muscles of the chicken (3, 4, 8), and the extraocular and intrinsic ear muscles of mammals (reviewed in ref. 9) that include both multi- and single-terminal fibers.

The present report focuses on the intrinsic muscles of the syrinx and combines techniques of immunocytochemistry to classify muscle fibers with techniques to visualize neuromuscular junctions.

The publication costs of this article were defrayed in part by page charge payment. This article must therefore be hereby marked "*advertisement*" in accordance with 18 U.S.C. §1734 solely to indicate this fact.

MATERIALS AND METHODS

Materials. All muscles were from male and female zebra finches in good health and full adult plumage.

Supernatants containing mouse monoclonal antibodies MF30, ALD66, ALD19, ALD58, MF1, and MF20 were generously provided by D. Fischman and D. M. Bader (Cornell University School of Medicine). Supernatants with monoclonal antibodies S58, F59, and II66 were generously provided by F. E. Stockdale (Stanford University). Polyclonal rabbit antiserum prepared against chicken neural cell adhesion molecule (N-CAM) was the generous gift of U. Rutishauser (Case Western Reserve University). This antiserum labeled a similar pattern of two high molecular mass bands of ≈200 kDa in immunoblots against Nonidet P-40 solubilized chicken and zebra finch brain. Immunoblots with Nonidet P-40-solubilized zebra finch ALD muscle showed a single discrete band of ≈130 kDa (data not shown). These differences in molecular mass between brain and muscle N-CAM are similar to those reported by other authors (10, 11).

Immunocytochemistry. Immunocytochemistry on frozen sections was carried out by standard techniques. Briefly, muscles of interest were dissected out from birds given an overdose of Chloropent (Fort Dodge) (0.1 ml). Muscles were stored at 4°C in balanced salt solution until all muscles were dissected. Muscles of interest were then sandwiched between two slices of pectoral muscle, embedded in a gel of gum tragacanth and saline, and rapidly frozen in a bath of isopentane cooled over liquid nitrogen (12). In general, several syrinxes and ALD and PLD muscles from the same birds were included in one sandwich for simultaneous sectioning. Sections were cut at 8–10 μm width on a cryostat (IEC Minotome) and collected onto room temperature chromalum-coated slides. After blocking nonspecific sites in 1% bovine serum albumin, sections were incubated in primary antibodies (1:10 for monoclonal supernatants or 1:500 for polyclonal serum). In some cases, sections were incubated in biotin-conjugated sheep anti-mouse IgG antibody (Amersham) as secondary antibody, washed, and then incubated in avidin/biotinylated peroxidase conjugate (Vectastain ABC Elite kit). These sections were then developed in diaminobenzidine (0.2 mg/ml), 0.006% hydrogen peroxide, nickel ammonium sulfate (5 μg/ml) in 150 mM Tris·HCl (pH 7.4), dehydrated in a graded series of ethanol, cleared in xylene, and mounted under Permount (Fisher). For double labeling with monoclonal and polyclonal antibodies, biotinylated sheep anti-mouse IgG (Amersham) and fluorescein isothiocyanate (FITC)-conjugated goat anti-rabbit IgG (Tago) were used as second antibodies. Sections were then incubated in Texas

Abbreviations: AChR, acetylcholine receptor; ALD, anterior latissimus dorsi muscle; α-BTX, α-bungarotoxin; ChE, cholinesterase; FITC, fluorescein isothiocyanate; N-CAM, neural cell adhesion molecule; PLD, posterior latissimus dorsi muscle.

red/streptavidin (Amersham), coverslipped under *p*-phenylenediamine (1 mg/ml), 50% (vol/vol) glycerol, 0.1 M sodium bicarbonate (pH 9.0), and viewed under fluorescence microscopy with filters appropriate for fluorescein and rhodamine (to view Texas red).

Visualization of End Plates. Double labeling of fiber type and end plates in sections was achieved by using FITC-conjugated α-bungarotoxin (FITC-α-BTX, 0.1 μg/ml; Sigma) to visualize the distribution of acetylcholine receptors (AChRs) and monoclonal antibody with Texas red/streptavidin as described above to identify fiber type.

Synapses were also visualized on muscle fibers dissociated after fixation. Whole muscles were removed and pinned in 128 mM dextrose/2 mM EDTA/90 mM sodium phosphate, pH 7.2. In some cases, muscles were fixed in −20°C methanol for 30 sec and then manually dissociated with tungsten wires. In other cases, muscles were fixed in 2% paraformaldehyde in the same buffer for 30 min over ice, rinsed, and carefully dissected away from any attached cartilage and connective tissue. Muscle fibers were then dissociated with a Brinkman Polytron (model PT10/35 with a PT10ST probe generator at setting 5.0) (13, 14). This device minces tissue by the shearing action of small blades, but it shears fixed muscle primarily between fibers. Muscles were dissociated for 15 or 30 sec in 2 ml of buffer, the Polytron bit was rinsed twice for 15 sec with 2 ml, and the 6 ml of fiber suspension were combined and stored at 4°C until processed further.

Dissociated fibers were then labeled with antibodies as described above except that fibers were labeled in suspension and washed by pelleting the fibers out of 1 ml of 0.1% bovine serum albumin in phosphate-buffered saline through a cushion of 50% glycerol in saline. For autoradiographic visualization of AChRs on dissociated fibers, fibers were incubated in suspension in 5 nM ^{125}I-labeled α-BTX in 0.1% bovine serum albumin (^{125}I-α-BTX, New England Nuclear, 5–20 mCi/mg; 1 Ci = 37 GBq). After labeling, fibers were washed as described above and then resuspended in NTB2 nuclear track emulsion (diluted 1:1 with 50% glycerol; Kodak; ref. 15). This suspension was then carefully spread onto microscope slides, chilled over ice, and air dried in the dark. Emulsion-coated slides were developed by standard procedures (16). To visualize junctional cholinesterase (ChE), fibers were dried onto microscope slides and stained with Karnovsky's stain (17).

RESULTS

Patterns of Terminals on Muscle Fibers. The distribution of silver grains seen in autoradiograms of dissociated fibers labeled with ^{125}I-α-BTX revealed a large amount of heterogeneity in the pattern of innervation of syringeal muscle fibers from both male and female birds. The majority of fibers had a single large dense cluster of silver grains (Fig. 1*a*), which in some cases formed a clear lattice-like pattern wrapping around the fiber. We never observed a fiber with one of these dense clusters, which also had other dense clusters, suggesting that fibers with these large terminals had only one end plate. Another less abundant class of fibers had smaller clusters of silver grains scattered along their lengths (Fig. 1*a*). Such fibers also had diffuse labeling over their entire surfaces. Dense clusters and diffuse labeling were not seen when competitors of α-BTX were used to block specific binding, indicating that this represents specific binding to AChRs.

The distribution of reaction product on dissociated syringeal muscle fibers stained for ChE is similar to the distribution of AChR. Most ChE stain appeared as isolated dense ramifications of finger-like projections that encircle single muscle fibers (Fig. 1*b*), suggesting a single nerve terminal. Other fibers had spots of dense ChE activity scattered along their surfaces, suggesting that these fibers had multiple terminals (Fig. 1*b*). A third and very rare class of end plates appeared as a single long track of reaction product resembling the Endbuschel terminal of frog muscles (ref. 9; data not shown).

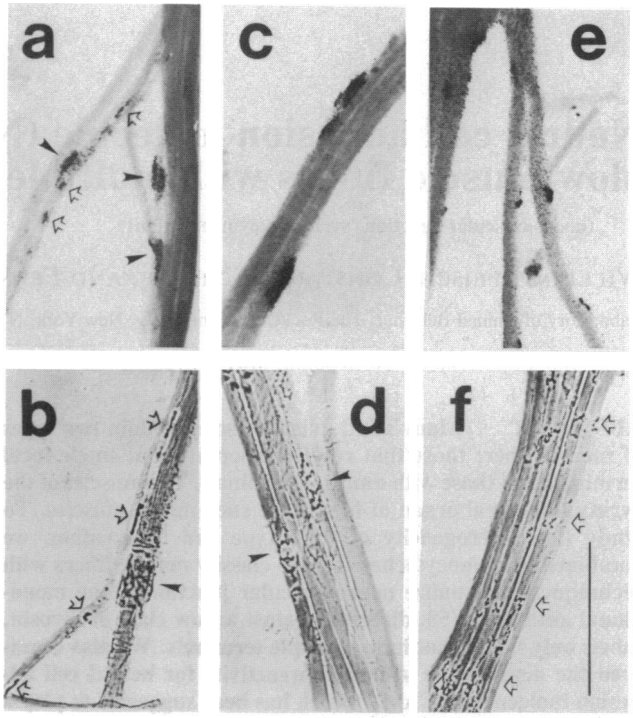

FIG. 1. AChR and ChE distribution on dissociated muscle fibers. Muscles were dissociated after paraformaldehyde fixation and fibers were labeled with ^{125}I-α-BTX and processed for autoradiography to visualize AChRs or stained for ChE as described. (*a*) Fibers from the syrinx of an intact male labeled to demonstrate AChRs, showing several fibers with densely labeled focal end plates (arrowheads) and a single fiber with scattered accumulations of label (arrows) and high extrajunctional labeling. (*b*) Syringeal fibers stained for ChE, with a focal end plate on one fiber (arrowhead) and scattered staining on an adjacent fiber (arrows). (*c*) α-BTX-labeled fibers from the hyomandibularis muscle, illustrating the densely labeled end plates characteristic of this muscle and of the PLD. (*d*) Fibers from the PLD muscle stained for ChE, with two characteristic focal end plates (arrowheads). (*e*) Fibers from the ALD muscle processed to demonstrate AChRs, showing the scattered terminals and high extrajunctional labeling characteristic of this muscle. (*f*) ALD fibers stained to demonstrate ChE, showing scattered terminals (arrows). (Bar = 200 μm.)

For comparison, we examined the pattern of α-BTX labeling and ChE staining on dissociated fibers from the ALD, the PLD, and the hyomandibularis muscles (18). Fibers of the PLD and most fibers of the hyomandibularis had single, large, isolated patches of AChR and ChE stain, resembling the patterns seen on most syringeal fibers and suggesting that these patches were indeed single discrete synapses (Fig. 1 *c* and *d*). In contrast, most fibers in the ALD preparation had diffuse scattered patches of AChR and ChE (Fig. 1 *e* and *f*), resembling the pattern seen on some syringeal fibers. ALD fibers also had a high density of extrajunctional AChRs, consistent with their diffuse sensitivity to acetylcholine (19).

Fiber Types. We screened 10 potentially useful antibodies (Table 1). Monoclonal antibodies specific for different isoforms of myosin or C-protein enabled us to identify at least four types of extrafusal muscle fibers. Monoclonal antibody MF30, raised against a fast myosin isoform (5), stains about half of the fibers in the fast-twitch PLD muscle and none of the fibers in the slow tonic ALD muscle. MF30-positive fibers were present in all of the muscles of the syrinx (Fig.

Table 1. Labeling of zebra finch muscles with antibodies

Antibody	Antigen	ALD	PLD	Syrinx
MF30	Neonatal fast myosin	−	++/−	++/−
ALD66	Slow C-protein	++	+/−	++/−
S58	Slow myosin	++	−	++/−
Polyclonal	N-CAM	++	−	+/−
ALD19	Slow myosin	−	+++	++
ALD58	Slow myosin	−	−	+
MF1	Fast C-protein	−	+++	+
F59	Fast myosin	++	++	++
MF20	Muscle myosin	++	++	++
II66	Surface glycoprotein	−	−	−

+/− indicates that the muscle is heterogeneous; some fibers are positively labeled and others are not. Antigens indicated were defined for chicken muscle and are only putative assignments for the zebra finch muscle used here.

2*a*), but the proportion of fibers stained in each of the muscles varies.

Monoclonal antibody ALD66 against a slow isoform of C-protein (5) labels zebra finch muscle in a pattern roughly complementary to that of MF30. It stained approximately half of the fibers of the PLD muscle and all of the fibers in the ALD (Table 1). In the syrinx as well, most fibers that were densely stained with ALD66 were not positive for MF30 (Fig. 2*b*).

A third monoclonal antibody, S58, specific for a slow isoform of myosin heavy chain (6), stained almost all fibers in the ALD and only intrafusal fibers in the PLD. In the syrinx, it stained a small proportion of fibers very intensely. None of these was organized in muscle spindles, which have not been found in syringeal muscle. One bundle of fibers within the dorsal muscle mass and adjacent to the syringeal lumen was made up predominantly of monoclonal antibody ALD-66-positive fibers and also had many fibers that were positive for monoclonal antibody S58 (Fig. 2 *b* and *c*). This bundle may correspond to the tracheobronchialis brevis described in other passerines (20).

The patterns of staining with these three monoclonal antibodies allowed us to distinguish at least three classes of muscle fibers in syringeal muscles: (*i*) those that were S58 positive, (*ii*) those that were ALD66 positive and S58 negative, and (*iii*) those that were MF30 positive (Fig. 2). Intrafusal muscle fibers of muscle spindles, which stain intensely with S58, were commonly seen in the PLD and pectoralis muscles but have not been found in syringeal muscles.

Double labeling with monoclonal antibody ALD66 and α-BTX revealed that many ALD66-positive fibers had large focal end plates characteristic of single-terminal fibers (Fig. 3 *a* and *b*). In contrast, no S58-positive fibers had single focal end plates. In preparations of dissociated fibers, S58-positive fibers had multiple terminals and most, and perhaps all, multiterminal fibers were S58 positive (Fig. 3 *c* and *d*).

N-CAM Immunoreactivity. We used fluorescent immunocytochemistry to localize N-CAM immunoreactivity in fresh frozen sections of muscle. As previously reported (11, 21), N-CAM was found to be colocalized with neuromuscular junctions, as visualized with α-BTX labeling (data not shown). N-CAM immunoreactivity was also patchily distributed around the perimeter of many muscle fibers (Fig. 4*b*). Since immunostaining was done with unfixed tissue, this patchy appearance may be due to antibody-induced redistribution of N-CAM. Some fibers had high levels of N-CAM immunoreactivity localized around their perimeter and throughout their interior (Figs. 4*b* and 5 *b* and *d*). Nonimmune rabbit serum produced no such pattern. The presence of N-CAM immunoreactivity within the confines of the sarcolemma is probably the result of N-CAM localization within the t-tubule system, which ramifies throughout the muscle fiber and is continuous with the extracellular surface (21).

Double labeling with anti-N-CAM and anti-slow myosin (S58) revealed that almost all fibers containing S58 immunoreactivity were also stained internally with anti-N-CAM (Figs. 4 and 5). A small proportion of fibers (<5%) were stained with S58, but not with anti-N-CAM, but all fibers that had clear internal staining with anti-N-CAM were S58 positive (Fig. 5 *c* and *d*).

DISCUSSION

Two patterns of innervation were found in the syringeal muscles of zebra finches: a single focal end plate type and a

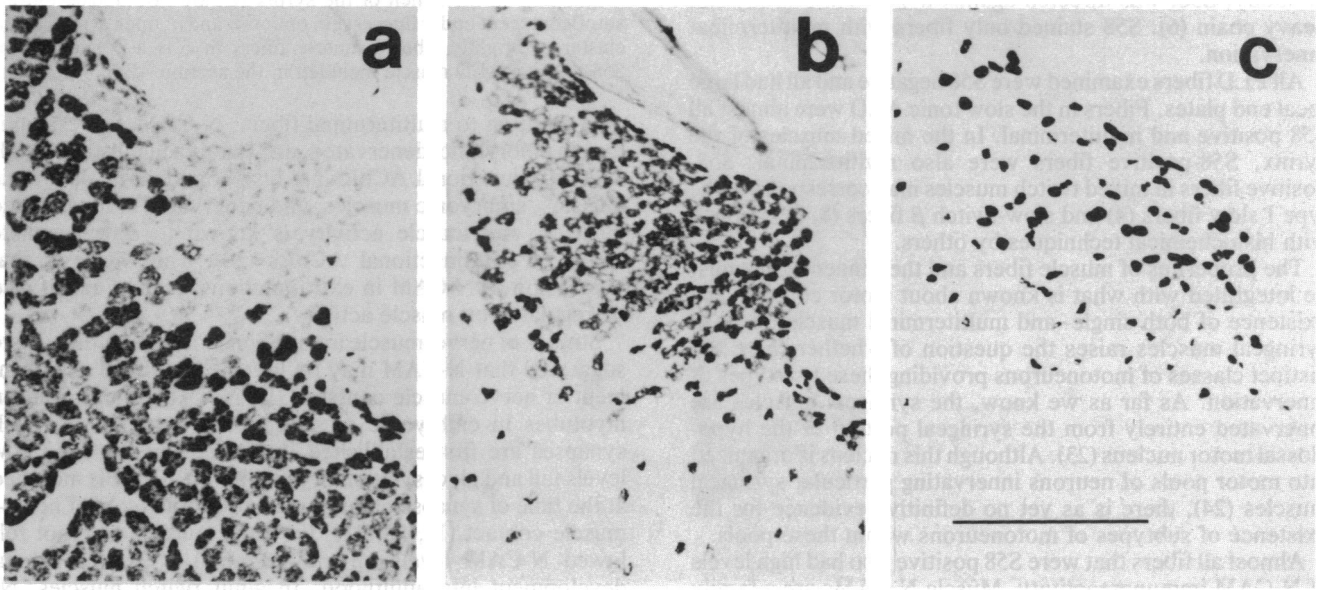

FIG. 2. Muscle fiber classes defined with monoclonal antibodies. Adjacent 8-μm cross-sections of a male zebra finch syrinx labeled with monoclonal antibody MF30 (*a*), ALD66 (*b*), and S58 (*c*) to demonstrate different fiber types. The deep fibers of the dorsal muscle bundle are shown. The lumen of the syrinx is in the upper right. Antibody was visualized with the avidin/biotin peroxidase complex method as described. (Bar = 200 μm.)

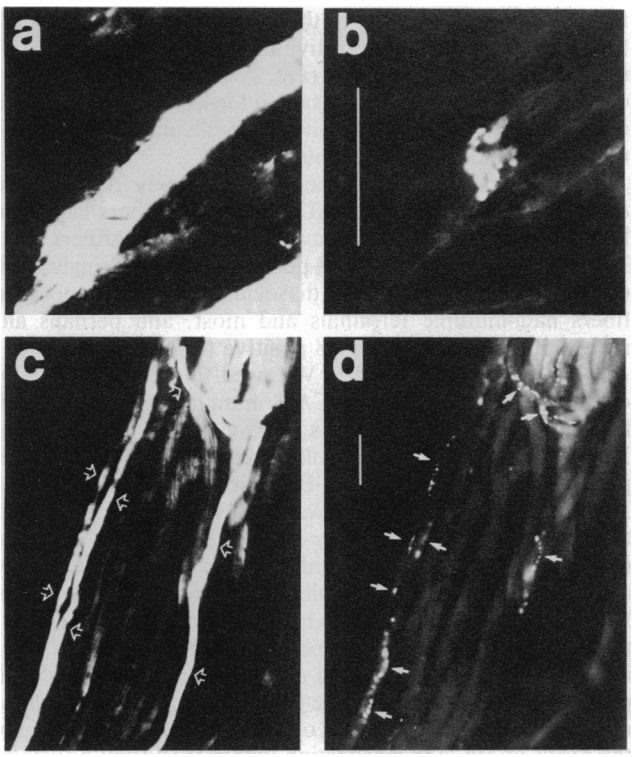

FIG. 3. Double labeling of muscle proteins and neuromuscular junctions. (*a* and *b*) Fresh frozen sagittal sections of syringeal muscle cut tangential to the fibers were double labeled with monoclonal antibody ALD66 against slow C-protein (*a*) and with FITC-α-BTX (*b*). An ALD66-positive muscle fiber in the center of the field (*a*) has a large end plate with the morphology typical of single focal terminals (*b*). (Bar = 40 μm.) (*c* and *d*) Syringeal muscles were manually dissociated after fixation in −20°C methanol. Fibers were double labeled with S58 to a slow myosin isoform (*c*) and with FITC-α-BTX (*d*) as described. S58-positive fibers (*c*; open arrows) have clusters of AChRs scattered along their surfaces, characteristic of multiple terminals (*d*; solid arrows). (Bar = 40 μm.)

multiterminal type. Only one of the antibodies that we screened had a clear association with innervation type. This antibody, S58, was directed against a slow class of myosin heavy chain (6). S58 stained only fibers with multiterminal innervation.

All PLD fibers examined were S58 negative and all had large focal end plates. Fibers in the slow tonic ALD were almost all S58 positive and multiterminal. In the mixed muscles of the syrinx, S58-positive fibers were also multiterminal. S58-positive fibers in mixed twitch muscles may correspond to the type I slow fibers (4) and slow-twitch β fibers (8, 22) defined with histochemical techniques by others.

The properties of muscle fibers and their innervation must be integrated with what is known about motor control. The existence of both single- and multiterminal muscle fibers in syringeal muscles raises the question of whether there are distinct classes of motoneurons providing these two types of innervation. As far as we know, the syringeal muscles are innervated entirely from the syringeal portion of the hypoglossal motor nucleus (23). Although this nucleus is organized into motor pools of neurons innervating particular syringeal muscles (24), there is as yet no definitive evidence for the existence of subtypes of motoneurons within these pools.

Almost all fibers that were S58 positive also had high levels of N-CAM immunoreactivity. Muscle N-CAMs are a family of high molecular weight glycoproteins, including membrane-bound and released forms (25, 26). N-CAM has been shown to be involved in a wide variety of cell–cell interactions (see refs. 27 and 28 for reviews).

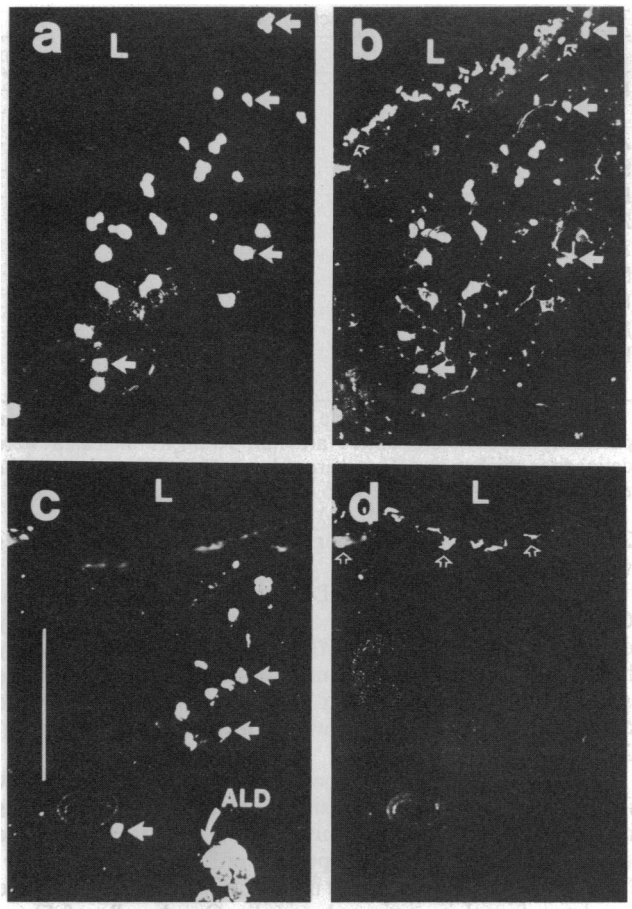

FIG. 4. Double labeling of slow myosin and N-CAM immunoreactivity. Cross-sections of syrinxes from adult zebra finches were labeled with S58 and visualized with rhodamine optics (*a* and *c*). These same sections were also incubated in the presence or absence of polyclonal anti-N-CAM and visualized under fluorescein optics (*b* and *d*). N-CAM immunoreactivity is patchily distributed around many muscle fibers that are S58 negative, and it is found within fibers that are S58 positive (*a* and *b*, solid arrows). In the absence of anti-N-CAM, no staining is observed in S58-positive fibers (*c* and *d*). Bright cells in the lumen of the syrinx (L) are not labeled but are autofluorescent under fluorescein optics (*b* and *d*; open arrows). The cluster of brightly labeled muscle fibers in *c* is a portion of the S58-positive ALD muscle included in the section. (Bar = 200 μm.)

In addition to multiterminal fibers, N-CAM expression is high in embryonic, denervated, and paralyzed muscle (10, 11, 29). Extrajunctional AChRs are also abundant in slow tonic muscles, embryonic muscles, and denervated and paralyzed muscles, and muscle activity is known to down-regulate levels of extrajunctional AChRs (30). This suggests that expression of N-CAM in extrajunctional regions might also be regulated by muscle activity.

Studies of nerve–muscle interaction in mixed cultures have suggested that N-CAM may be involved in initial establishment of nerve–muscle contact (31). N-CAM is abundant on myotubes in embryonic muscle during the time at which synapses are first established. In twitch muscles, N-CAM levels fall and glycosylation of remaining N-CAM is modified at the time of synapse elimination and stabilization of nerve–muscle contact (11, 32, 33). Previous studies have not followed N-CAM levels on multiterminal fibers throughout development into adulthood. In adult twitch muscles, N-CAM is low or undetectable on most of the sarcolemma, but it is localized at the neuromuscular junction (10, 11, 34). After denervation or paralysis of muscle, N-CAM accumulates throughout these muscles, and after reinnervation or recov-

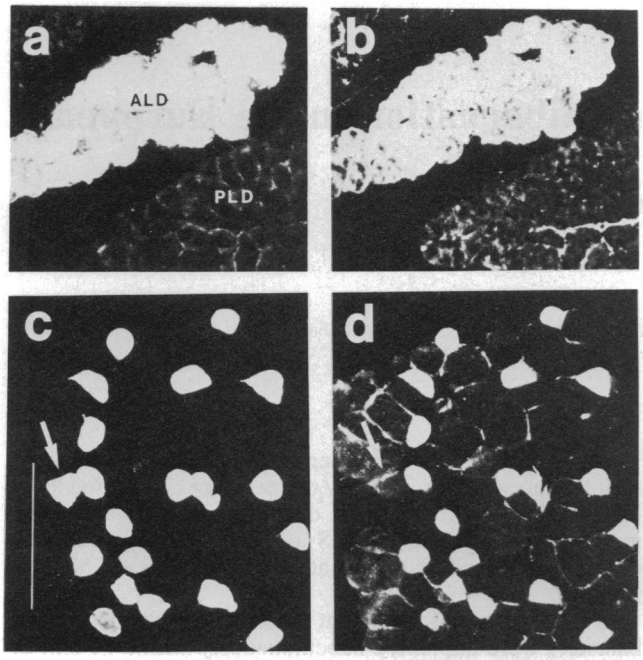

FIG. 5. Double labeling of slow myosin and N-CAM immunoreactivity. As in Fig. 4, cross-sections of zebra finch muscles were labeled with S58 (*a* and *c*) and polyclonal antibody anti-N-CAM (*b* and *d*). The ALD and PLD muscles are shown in *a* and *b*. The ALD, a slow tonic muscle, is S58 positive and expresses high levels of N-CAM, while the adjacent PLD, a fast-twitch muscle, is S58 negative and has low N-CAM expression. (*c* and *d*) The trapezius (18) is shown. This mixed muscle of the dorsal trunk with fiber types intermingled shows clear colocalization of slow myosin (*c*) and N-CAM (*d*) immunoreactivity. One fiber, which is S58 positive but N-CAM negative, is designated by an arrow.

ery the low levels of N-CAM normally found in adult twitch muscle are reestablished (10). Thus, the pattern of N-CAM abundance parallels the susceptibility of muscle to innervation. This pattern is distinct from the pattern of accumulation of several other molecules implicated in cell–cell and cell–substrate interactions (34). Recent experiments suggest that, while N-CAM may not be required for formation of functional neuromuscular junctions (35, 36), it may play a role in determining and stabilizing the pattern of muscle innervation (33, 37, 38). The presence of high levels of N-CAM immunoreactivity on most and perhaps all multiterminal muscle fibers suggests an additional hypothesis; that high levels of N-CAM on these fibers may play a role in maintenance of the multiterminal pattern of innervation in certain adult muscle fibers. If N-CAM on the surface of multiterminal fibers continues to attract innervation or permits new terminals to form outside of existing junctions, a pattern of multiple terminals might be the result. The pattern of terminals seen at any one time on these fibers might be unstable as new terminals constantly form and old ones retract.

The authors thank David M. Bader, Donald Fischman, Urs Rutishauser, and Frank E. Stockdale for generously providing antibodies. Urs Rutishauser and Arlene Chiu provided helpful comments and criticisms. This work was supported by Grant PHS MH18343 from the National Institutes of Health and by Biomedical Research Support Grant SO7 RR07065. W.B. was supported by a Norman and Rosita Winston Fellowship.

1. Kuffler, S. W. & Vaughan-Williams, E. M. (1953) *J. Physiol. (London)* **121,** 289–317.
2. Kruger, P. & Gunther, P. G. (1958) *Acta Anat.* **33,** 325–338.
3. Ginsborg, B. L. (1960) *J. Physiol. (London)* **154,** 581–598.
4. Barnard, E. A., Lyles, J. M. & Pizzey, J. A. (1982) *J. Physiol. (London)* **331,** 333–354.
5. Reinach, F. C., Masaki, T., Shafiq, S., Obinata, T. & Fischman, D. A. (1982) *J. Cell Biol.* **95,** 78–84.
6. Miller, J. B., Crow, M. T. & Stockdale, F. E. (1985) *J. Cell Biol.* **101,** 1643–1650.
7. Ginsborg, B. L. & Mackay, B. (1961) *Bibl. Anat.* **2,** 174–181.
8. Ashmore, C. R., Kikuchi, T. & Doerr, L. (1978) *Exp. Neurol.* **58,** 272–284.
9. Hess, A. (1970) *Physiol. Rev.* **50,** 40–62.
10. Covault, J. & Sanes, J. R. (1985) *Proc. Natl. Acad. Sci. USA* **82,** 4544–4548.
11. Rieger, F., Grumet, M. & Edelman, G. M. (1985) *J. Cell Biol.* **101,** 285–293.
12. Dubowitz, V. (1985) *Muscle Biopsy: A Practical Approach* (Saunders, Philadelphia), pp. 13–19.
13. Robbins, N., Olek, A., Kelly, S. S., Takach, P. & Christopher, M. (1980) *Proc. R. Soc. London Ser. B* **209,** 555–562.
14. Steinbach, J. H. (1981) *Dev. Biol.* **84,** 267–276.
15. Kopriwa, B. M. & Moss, F. P. (1971) *J. Histochem. Cytochem.* **19,** 51–55.
16. Rogers, A. W. (1979) *Techniques of Autoradiography* (Elsevier, Amsterdam), 3rd Ed., pp. 351–368.
17. Karnovsky, M. J. (1964) *J. Cell Biol.* **23,** 217–232.
18. Chamberlain, F. W. (1943) *Atlas of Avian Anatomy: Osteology, Arthrology, Myology* (Hallenbeck, Lansing, MI), pp. 154–169 and 206–209.
19. Fedde, M. R. (1969) *J. Gen. Physiol.* **53,** 624–637.
20. Warner, R. W. (1972) *J. Zool. (London)* **168,** 381–393.
21. Covault, J. & Sanes, J. R. (1986) *J. Cell Biol.* **102,** 716–730.
22. Ashmore, C. R. & Doerr, L. (1971) *Exp. Neurol.* **30,** 431–446.
23. Nottebohm, F., Stokes, T. M. & Leonard, C. M. (1976) *J. Comp. Neurol.* **165,** 457–486.
24. Vicario, D. S. & Nottebohm, F. (1988) *J. Comp. Neurol.* **271,** 346–354.
25. Covault, J., Merlie, J. P., Goridis, C. & Sanes, J. R. (1986) *J. Cell Biol.* **102,** 731–739.
26. Dickson, G., Gower, H. J., Barton, C. H., Prentice, H. M., Elsom, V. L., Moore, S. E., Cox, R. D., Quinn, C., Putt, W. & Walsh, F. S. (1987) *Cell* **50,** 1119–1130.
27. Edelman, G. M. (1986) *Annu. Rev. Cell Biol.* **2,** 81–116.
28. Rutishauser, U., Acheson, A., Hall, A. K., Mann, D. M. & Sunshine, J. (1988) *Science* **240,** 53–57.
29. Kay, B. K., Schwartz, L. M., Rutishauser, U., Qiu, T. H. & Peng, H. B. (1988) *Development* **103,** 463–472.
30. Lomo, T. & Westgaard, R. H. (1975) *J. Physiol. (London)* **252,** 603–626.
31. Rutishauser, U., Grumet, M. & Edelman, G. M. (1983) *J. Cell Biol.* **97,** 145–152.
32. Moore, S. E. & Walsh, F. S. (1985) *EMBO J.* **4,** 623–630.
33. Tosney, K. W., Watanabe, M., Landmesser, L. & Rutishauser, U. (1986) *Dev. Biol.* **114,** 437–452.
34. Sanes, J. R., Schachner, M. & Covault, J. (1986) *J. Cell Biol.* **102,** 420–431.
35. Bixby, J. L. & Reichardt, L. F. (1987) *Dev. Biol.* **119,** 363–372.
36. Mehrke, G., Jockusch, H. & Schachner, M. (1987) *Neurosci. Lett.* **78,** 247–252.
37. Rieger, F., Nicolet, M., Pinçon-Raymond, M., Murawsky, M., Levi, G. & Edelman, G. M. (1988) *J. Cell Biol.* **107,** 707–720.
38. Landmesser, L., Dahm, L., Schultz, K. & Rutishauser, U. (1988) *Dev. Biol.* **130,** 645–670.